



POLITÉCNICA

# Assessment of fissionable material behaviour in fission chambers

**O. Cabellos, P. Fernández, N. García-Herranz**  
*Universidad Politécnica de Madrid (UPM)*

**D. Rapisarda**  
*CIEMAT*

*JEFF/EFF Meeting*  
31 May – 2 June 2010  
NEA, Issy-les-Moulineaux, France

# OUTLINE

## **PART I: Introduction**

## **PART II: Computation of the reaction rates in a fission chamber and its sensitivity to neutron spectrum**

- **Reaction rates and saturation current delivered by a fission chamber**
- **Sensitivity of the saturation current with respect to the neutron spectrum**

## **PART III: Other parameters having influence on the fission chamber behaviour**

- **Total radioactivity**
- **Xenon inventory**
- **Temperature effect**
- **Deposit thickness**

## **PART IV: Impact of activation cross section uncertainties**

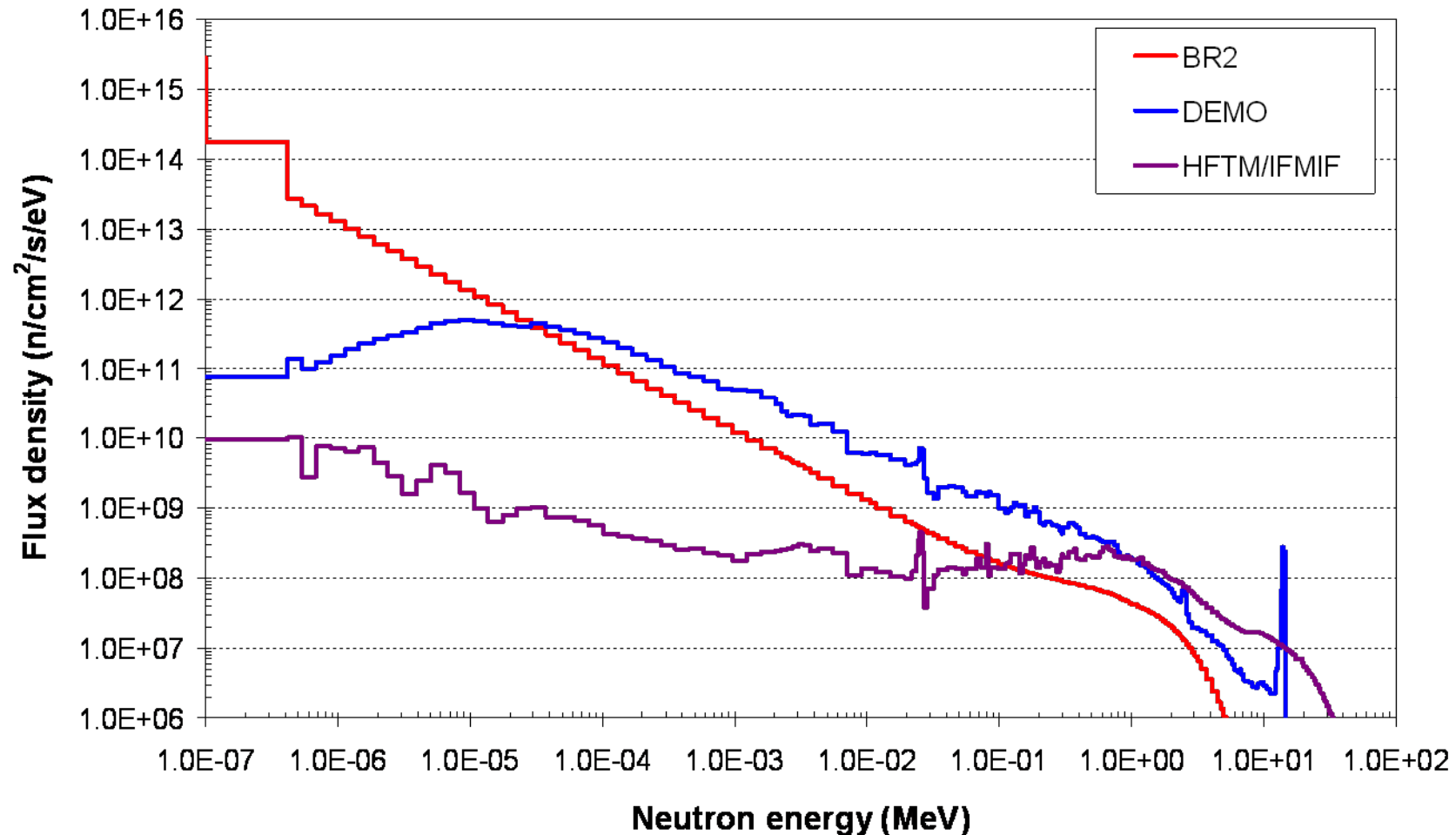
## **CONCLUSIONS**

# INTRODUCTION

- ✚ A comprehensive study is performed in order to assess the pertinence of fission chambers coated with different fissile materials for high neutron flux detection
- ✚ Three neutron scenarios are proposed to study the fast component of a high neutron flux:
  - ✚ High neutron flux with a significant thermal contribution such as BR2
  - ✚ DEMO magnetic fusion reactor
  - ✚ IFMIF high flux test module
- ✚ In this study, the inventory code ACAB (NEA-1839) is used to analyze the following questions:
  - ✚ Impact of different deposits in fission chambers
  - ✚ Effect of the irradiation time/burn-up on the concentration
  - ✚ Impact of activation cross section uncertainties on the composition of the deposit for all the range of burn-up/irradiation neutron fluences of interest
- ✚ **The complete set of nuclear data (decay, fission yield, activation cross sections and uncertainties) provided by EAF2007 data library are used for this evaluation.**

# PART I: Introduction: Neutron scenarios

**Figure 1.** Neutron spectra of different neutron environments in a VITAMIN-J+ (211) multi-group structure.



## PART II: Reaction rates and sensitivity to neutron spectrum

**Table I.** Total neutron flux and fraction of neutrons in four energy ranges for the three neutron scenarios.

	% neutrons having energies				Total neutron flux (x 10 <sup>14</sup> ) (n/cm <sup>2</sup> /s)
	E <0.625eV= E <sub>0</sub> thermal	E <sub>0</sub> < E <1 MeV epithermal	1 MeV < E <20 MeV fast	E >20 MeV extended	
BR2	55.53	35.99	8.48	-	6.16
DEMO	0.00	66.72	33.28	-	13.0
IFMIF/HFTM	0.00	27.28	66.53	6.19	7.30

The total neutron flux can be decomposed into four components as follows:

$$\phi_{total} = \sum_g \phi_g = \sum_{I=ther, epi, \dots} \left( \sum_{g \in G_I} \phi_g \right) = \sum_I \phi_I = \phi_{thermal} + \phi_{epi} + \phi_{fast} + \phi_{extended}$$

The collapsed one group cross section with a multigroup neutron spectrum is written as:

$$\frac{\sum_{g \in G_I} \sigma_g \phi_g}{\sum_g \phi_g} = \frac{\sum_{g \in G_I} \sigma_g \phi_g}{\phi^{total}} = \bar{\sigma}_I$$

The total fission reaction rate for a given neutron spectrum and for a given fissile deposit target can be computed as:

$$R_{tot}(t) = \sum_i N^i(t) \bar{\sigma}_{fiss}^i \phi_{total}$$

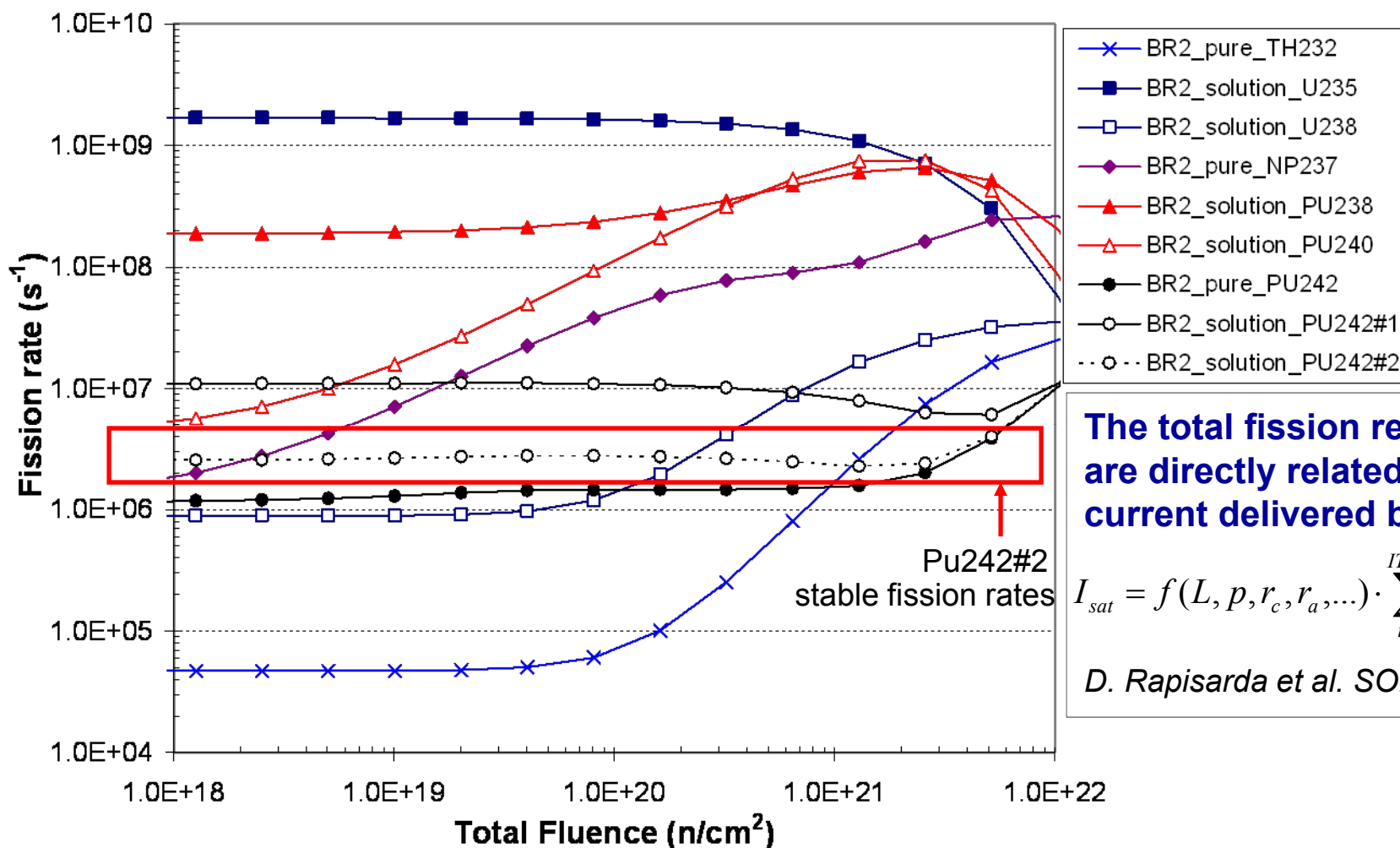
## PART I: Introduction: Other realistic fissile deposits?

**Table II.** Isotopic composition of the potential fissile deposit or solutions.

Deposit	Mass (μg)	Atomic percentage in %									
		<sup>232</sup> Th	<sup>235</sup> U	<sup>238</sup> U	<sup>237</sup> Np	<sup>238</sup> Pu	<sup>239</sup> Pu	<sup>240</sup> Pu	<sup>241</sup> Pu	<sup>242</sup> Pu	<sup>244</sup> Pu
Th232	3.85	100									
U235	3.90		97	3							
U238	3.95		0.04	99.96							
Np237	3.93				100						
Pu238	3.95					94.95	4.58	0.40	0.02	0.05	
Pu240	3.98					0.02	0.08	99.88	-	0.02	
Pu242	4.02									100	
Pu242 #1	4.02					0.214	0.116	0.172	0.180	99.274	0.044
Pu242 #2	4.02					0.004	0.005	0.022	0.035	99.932	0.002

## PART II: Reaction rates

**Figure 2.** Fission rates (fission/s) for the different pure and solution deposits in a typical high flux thermal neutron environment (BR2).



**The total fission reaction rates are directly related with the current delivered by the FC:**

$$I_{sat} = f(L, p, r_c, r_a, \dots) \cdot \sum_{i=1}^{ITOT} N^i(t) \bar{\sigma}_{fission}^i \phi_{total}$$

*D. Rapisarda et al. SOFT2010*

## PART II: Sensitivity to neutron spectrum

We define the relative change in the saturation current (under flux variations ) as:

$$\frac{\Delta I_{sat}}{I_{sat}} = \sum_{I=ther, epi, \dots} \left( \left. \frac{\partial I_{sat}}{\partial \phi_I} \right|_{\phi \neq \phi_I, cte} \frac{\phi_I}{I_{sat}} \right) \frac{\Delta \phi_I}{\phi_I} = \sum_{I=ther, epi, \dots} S_I \frac{\Delta \phi_I}{\phi_I}$$

The sensitivity coefficient of the current with respect to a flux variation is

$$S_I = \left. \frac{\partial I_{sat}}{\partial \phi_I} \right|_{\phi \neq \phi_I, cte} \frac{\phi_I}{I_{sat}} = \left( \sum_i N^i \hat{\sigma}_I^i \right) \frac{\phi_I}{R_{tot}} = \frac{R_I}{R_{tot}} \quad \text{with: } \sum_I S_I = 1$$

The fission reaction rates in each energy-region can be defined by

$$R_I = \sum_i N^i \left( \sum_{g \in G_I} \sigma_g^i \phi_g \right) = \sum_i N^i \hat{\sigma}_I^i \phi_I = \sum_i N^i \bar{\sigma}_I^i \phi_{total}$$

In the case of an impure deposit, we define  $S_I$  as:  $S_I = \sum_k \alpha_k S_I^k \beta_k$

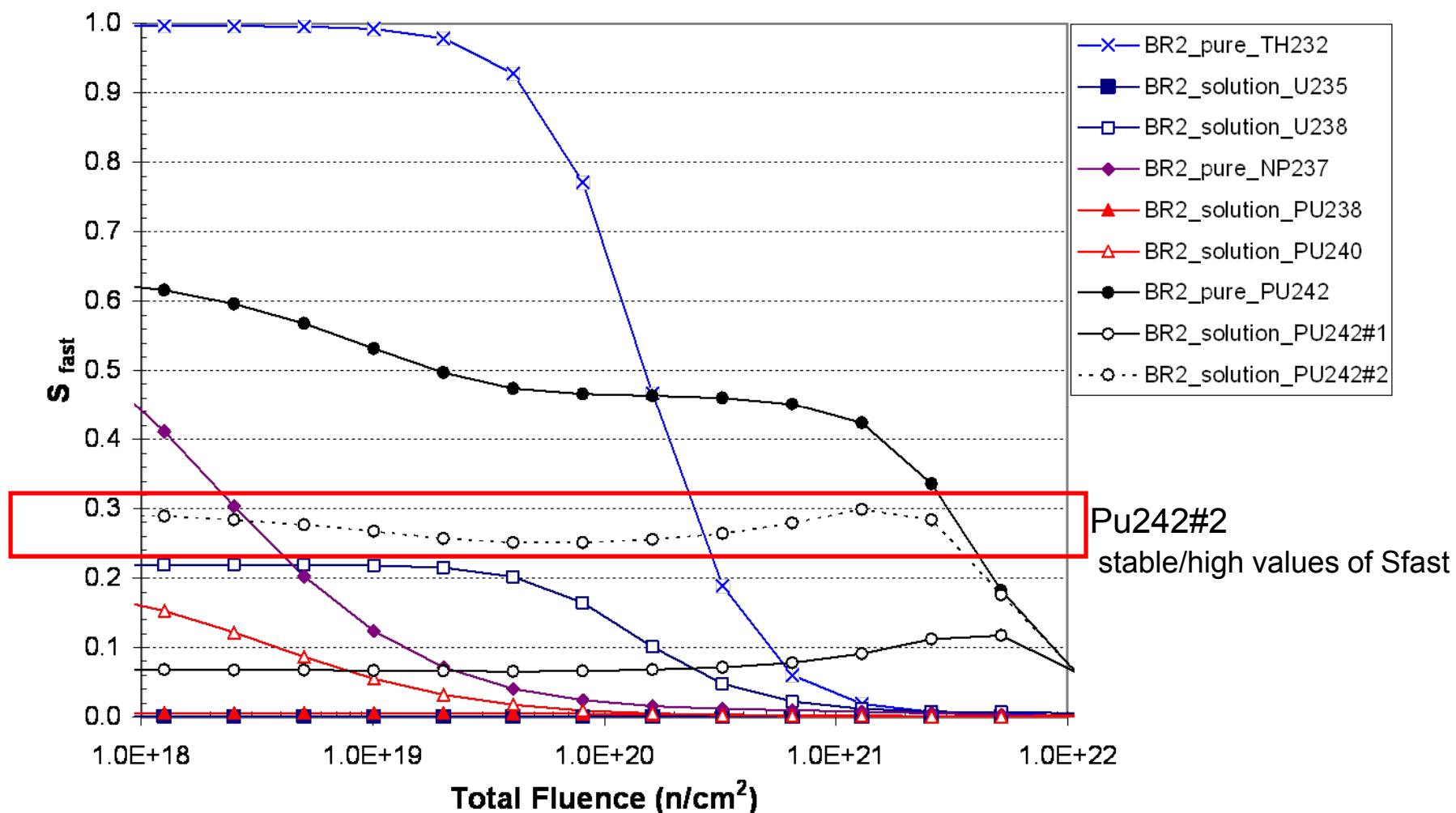
where:

- $\alpha_k$  is the atomic percentage of the pure deposit  $k$
- $S_I^k$  is the sensitivity of the pure deposit  $k$
- $\beta_k$  is  $R^k/R_{tot}$ , the relative fraction of fission rate of the pure deposit  $k$



## PART II: Sensitivity to neutron spectrum

**Figure 4.** Sensitivity to fast neutrons for initially different pure and solution deposits in a typical high flux thermal neutron environment (BR2).



# PART III: Other parameters having influence in FC behaviour

## + Total radioactivity

- + Evolution of total activity induced in the FC (waste management)

## + Xenon inventory

- + Addition of contaminants with low ionization potential (e.g. Xenon ~ 0.1%)

## + Deposit thickness

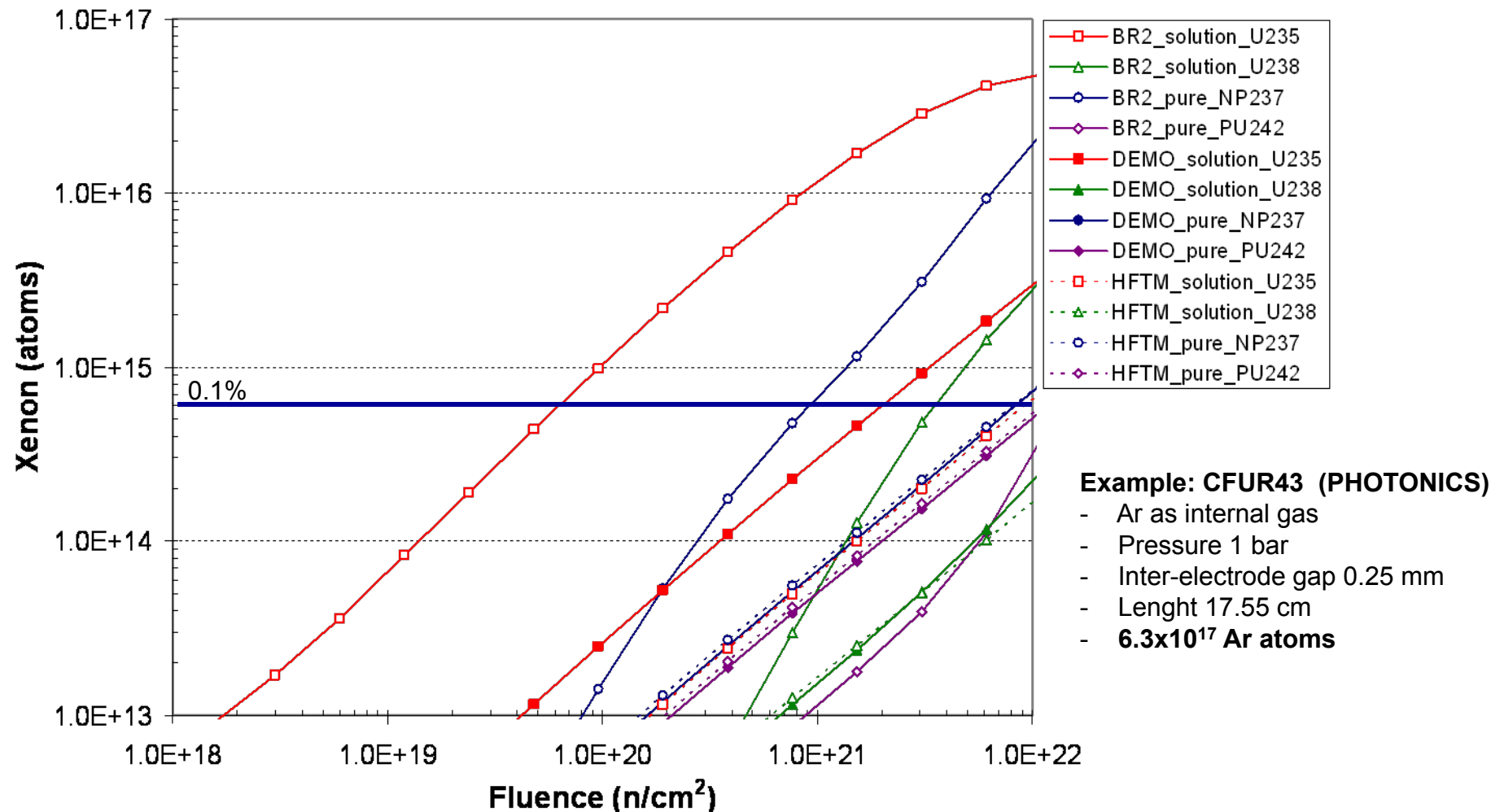
- + To analyze the self-shielding phenomenon:  $\delta^{\max} < \varepsilon / \Sigma_{total}$
- + To assess the fission product trapping within the deposit (auto-absorption)

## + Temperature effect

- + We assess the temperature effect for different deposits irradiated in BR2
- + Two sets of calculations have been performed:
  - + “**BRANCHING**” cases, the reference temperature of 325K used is instantaneously changed to 350K at each irradiation time. Assuming a constant total neutron flux, the differences in the total fission rates are due to the different one-group fission cross sections (each one collapsed with a different spectrum).
  - + “**SPECTRAL HISTORY**” cases, “SH”, we keep the temperature at 350K during the whole irradiation time, so not only the one-group fission cross sections change, but also the atomic concentration.

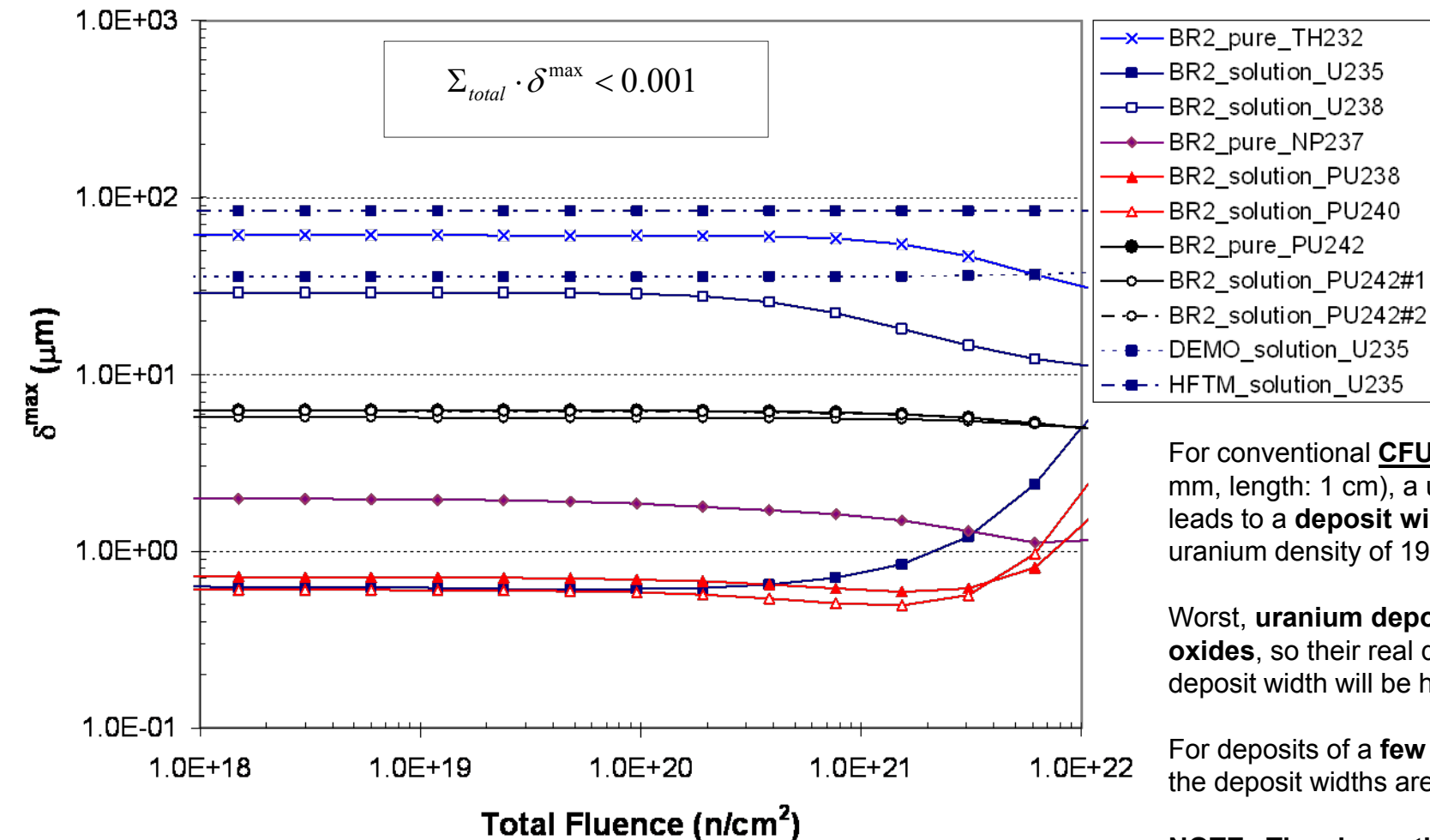
## PART III: Xenon

**Figure 5.** Contamination of the filling gas by Xenon (atoms) induced in the fission chamber for initially different pure (Np237 and Pu242) and solution (U235 and U238) deposits in typical high neutron flux environments



## PART III: Self-shielding phenomenon

**Figure 6.** Predicted maximum thickness assuming an interaction probability ( $\varepsilon$ ) of 0.001



For conventional **CFUT-C3** anodes (radius: 1.25 mm, length: 1 cm), a uranium deposit of **3 g** leads to a **deposit width of 1.3 mm**, with a uranium density of  $19.1 \text{ g}/\text{cm}^3$ .

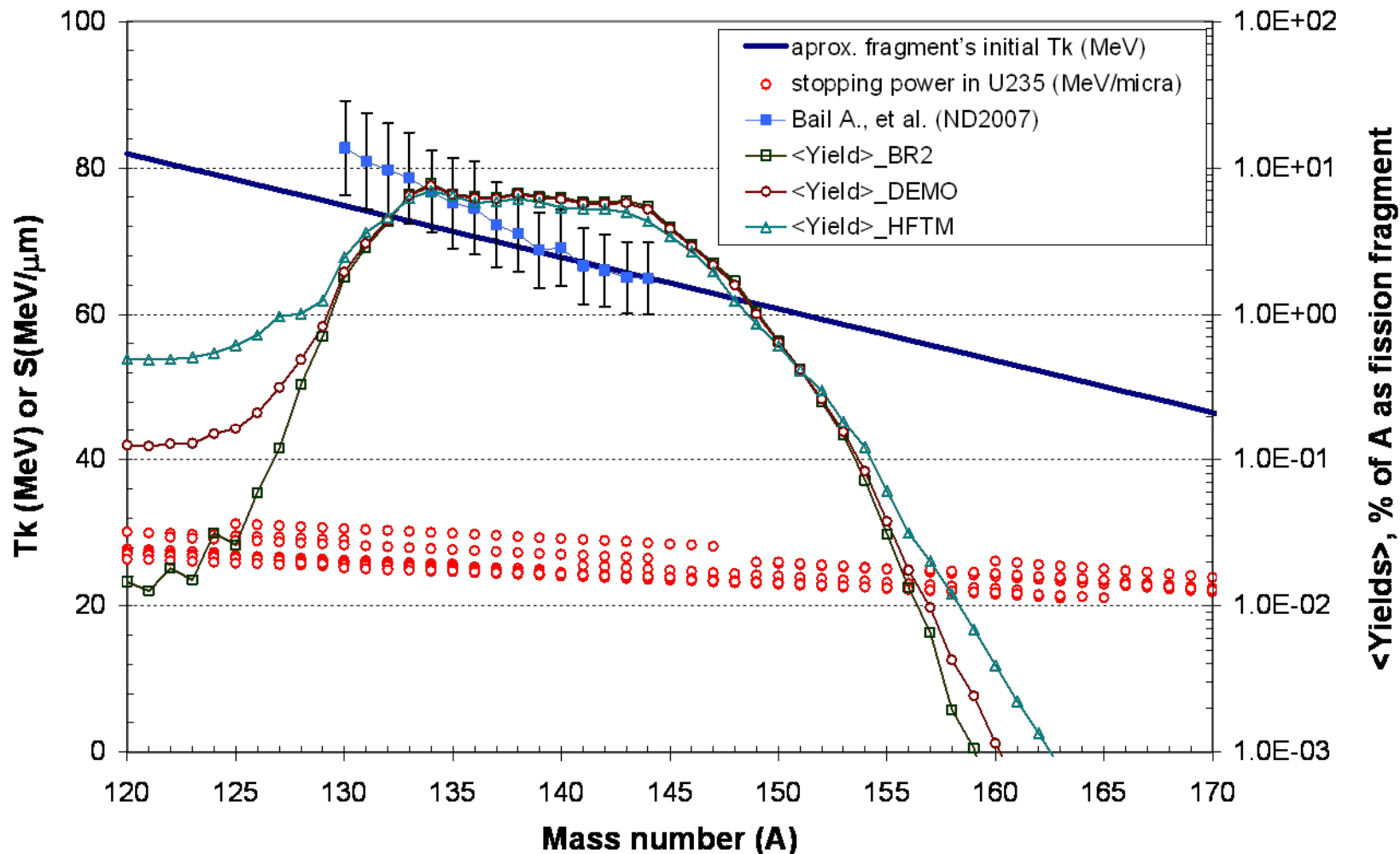
Worst, **uranium deposits are essentially oxides**, so their real density is lower and the deposit width will be higher.

For deposits of a **few micrograms**, however, the deposit widths are around **1 nm**.

**NOTE:** The absorption of FPs within the **deposit** could become non negligible for large deposits of a few grams.

## PART III: Fission product trapping within the deposit

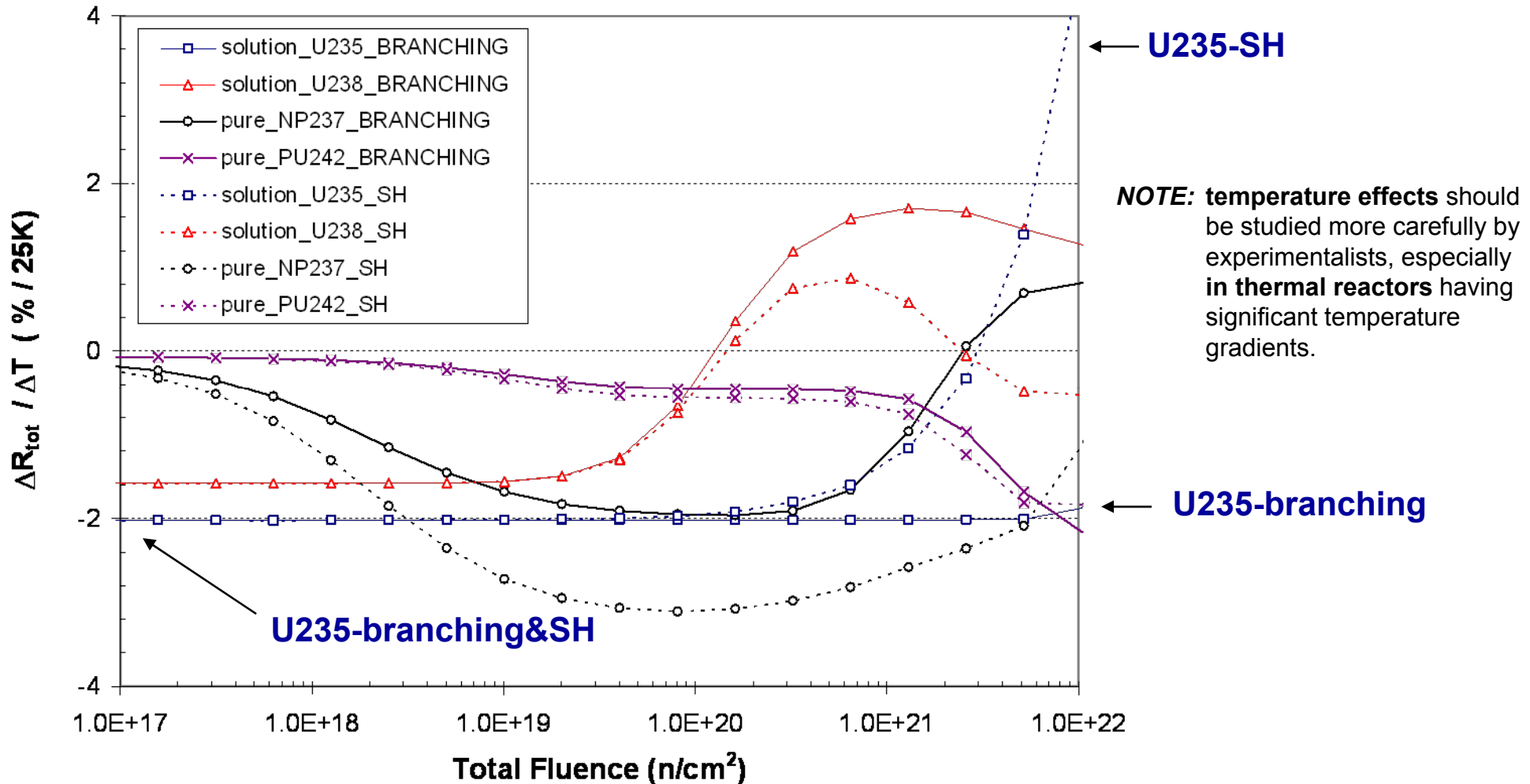
**Figure 7.** On the left axis, the roughly total kinetic energy of any fragment with mass number A, mean and relative error kinetic energy (one standard deviation) from fission of  $^{235}\text{U}(\text{nth},\text{f})$  taken from [14] and the stopping power ( $\text{MeV}/\mu\text{m}$ ) at this energy calculated with SRIM in Uranium for different elements (charge Z) with the same mass number.



On the right axis, the effective fission product yield for  $^{235}\text{U}$  collapsed by ACAB code for different neutron spectra.

# PART III: Temperature effect: Branching/Spectral History cases

**Figure 8.** Temperature dependence of the fission rates for different deposits.



- **Branching cases** show the difference in % between a reference irradiation case at 325K and an instantaneous change in the temperature of +25K
- **Spectral history cases:** we compare the nominal case at 325K with a modified irradiation case at 350K

## PART IV: Impact of activation cross section uncertainties

**Table III.** Total relative experimental error (in %) for capture and fission cross sections from EAF2007/UN.

	Fission			Capture		
	BR2	DEMO	HFTM	BR2	DEMO	HFTM
<b>Th232</b>	16.6	16.7	13.7	2.5	3.8	15.4
<b>U235</b>	3.1	7.0	15.1	3.0	4.8	15.5
<b>U238</b>	16.6	16.7	13.9	2.8	3.3	13.5
<b>Np237</b>	15.8	16.6	15.4	3.2	7.6	15.0
<b>Np238</b>	46.7	24.7	30.7	33.0	24.5	32.3
<b>Pu238</b>	5.4	12.5	15.6	3.9	10.0	15.9
<b>Pu239</b>	3.3	6.0	15.3	4.5	8.6	14.3
<b>Pu240</b>	14.0	16.2	14.9	2.5	3.5	7.8
<b>Pu241</b>	3.3	8.8	15.1	3.0	8.0	16.3
<b>Pu242</b>	14.8	16.5	15.2	8.0	8.0	14.0
<b>Pu243</b>	118.4	47.67	59.5	274.6	23.6	32.4
<b>Pu244</b>	16.5	16.6	15.2	15.1	23.9	32.6

Given  $\mathbf{V}$  the G-by-G variance matrix of the relative cross sections vector, the variance  $\Delta^2$  of the relative spectrum-averaged cross section is:

$$\Delta^2 = \omega^T \mathbf{V} \omega$$

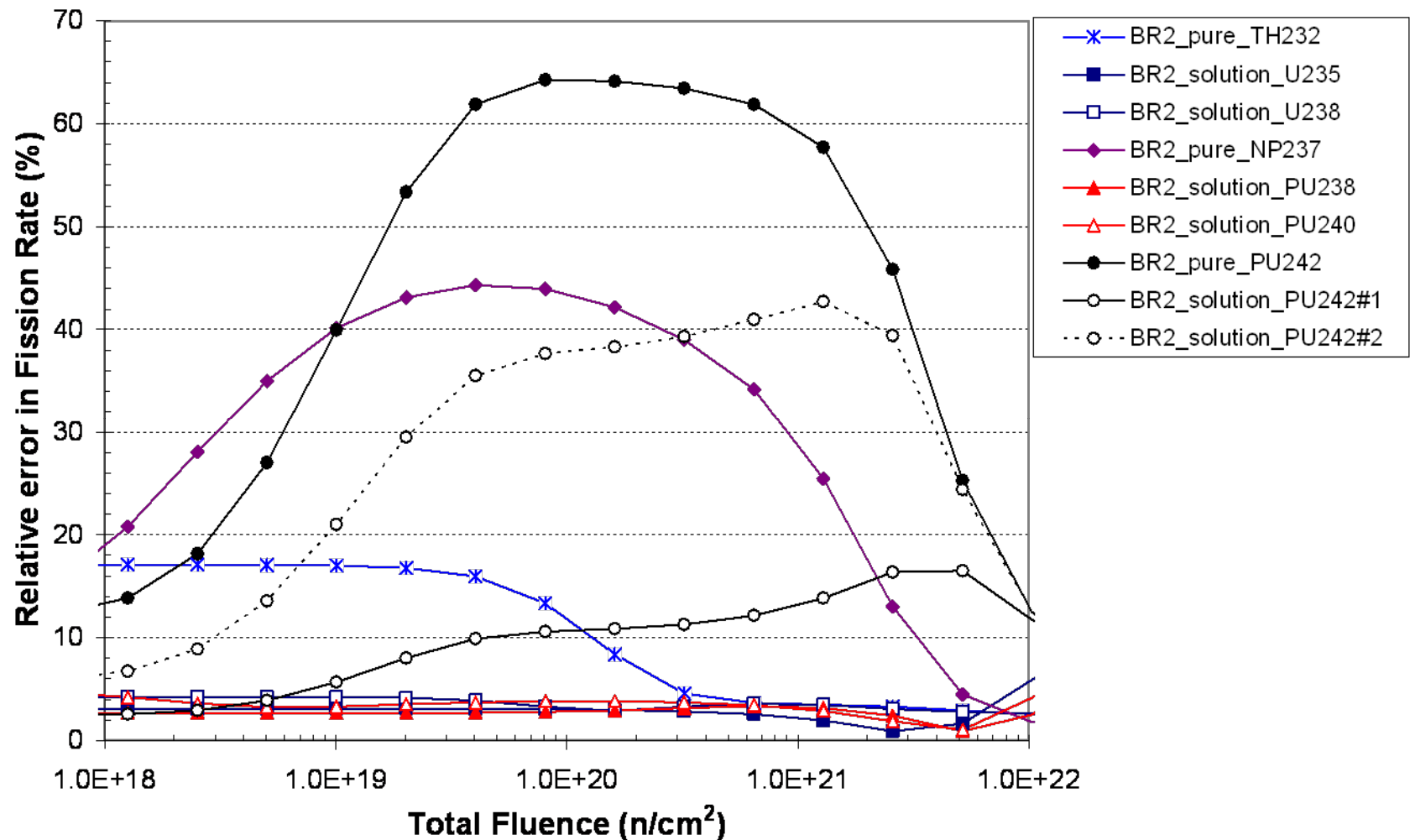
$$\text{with: } \omega = \left[ \frac{\phi_1}{\bar{\phi}} \frac{\sigma_1}{\sigma^{eff}}, \dots, \frac{\phi_G}{\bar{\phi}} \frac{\sigma_G}{\sigma^{eff}} \right]^T$$

the total flux as:  $\bar{\phi} = \phi_1 + \phi_2 + \dots + \phi_G$

$$\text{and: } \sigma^{eff} = \frac{\phi_1 \sigma_1 + \phi_2 \sigma_2 + \dots + \phi_G \sigma_G}{\phi_1 + \phi_2 + \dots + \phi_G}$$

## PART IV: Relative error in fission rates in BR2

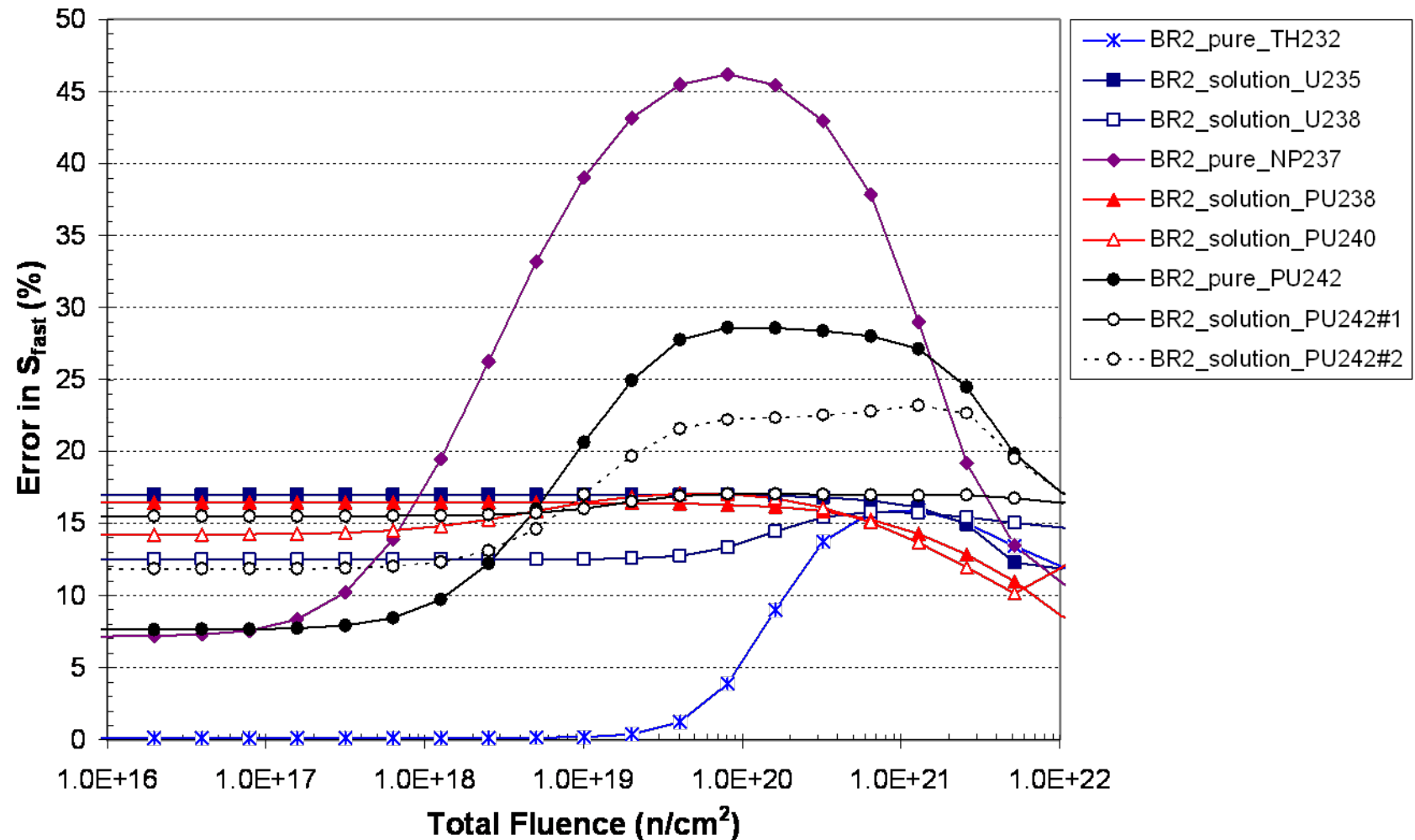
**Figure 9.** Relative error in fission rates (in %) for different pure and solution deposits in a typical high flux thermal neutron environment (BR2).





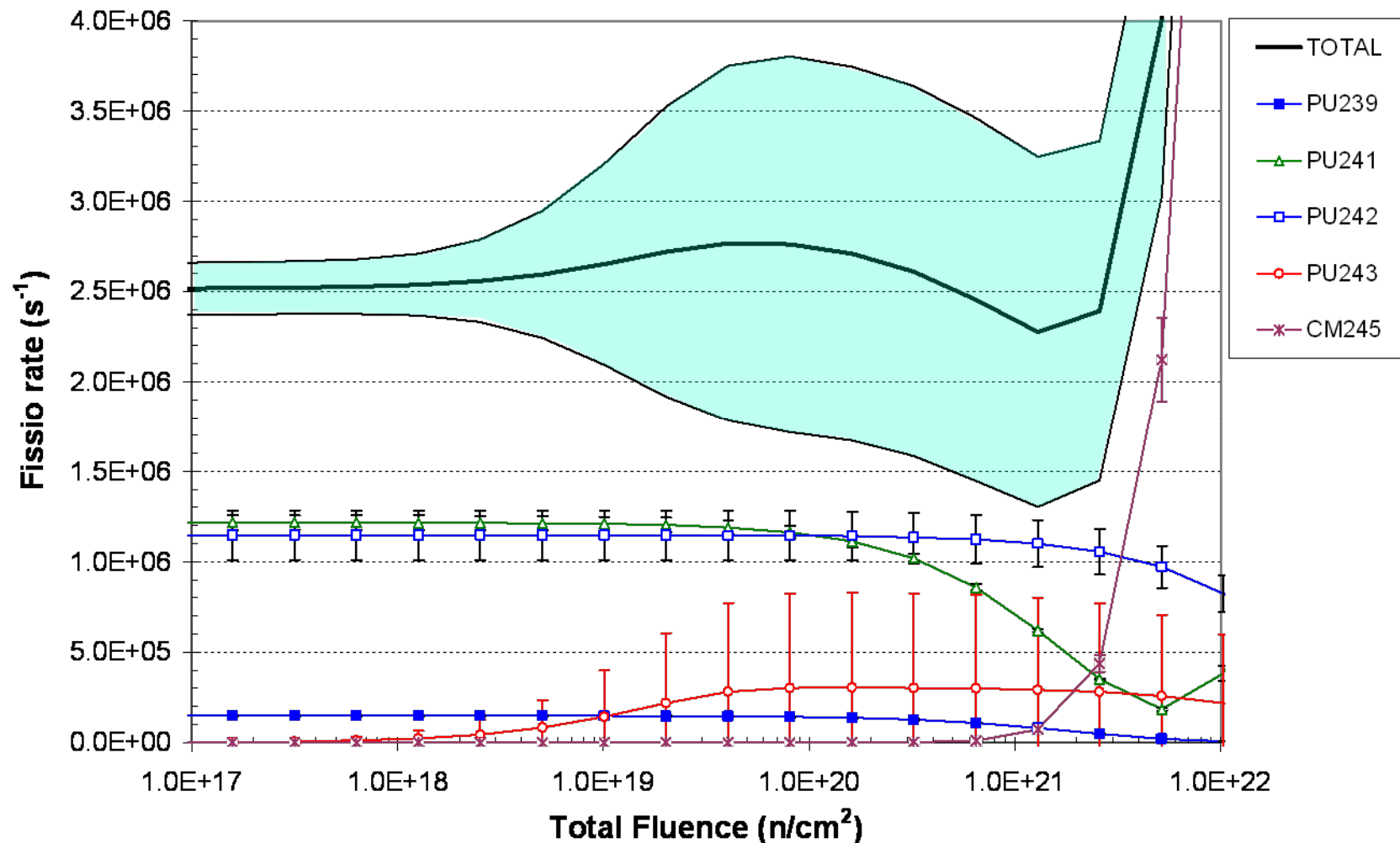
## PART IV: Relative error in S<sub>fast</sub> in BR2

**Figure 10.** Relative error in Sensitivity to fast neutrons (in %) for different pure and solution deposits in a typical high flux thermal neutron environment (BR2).



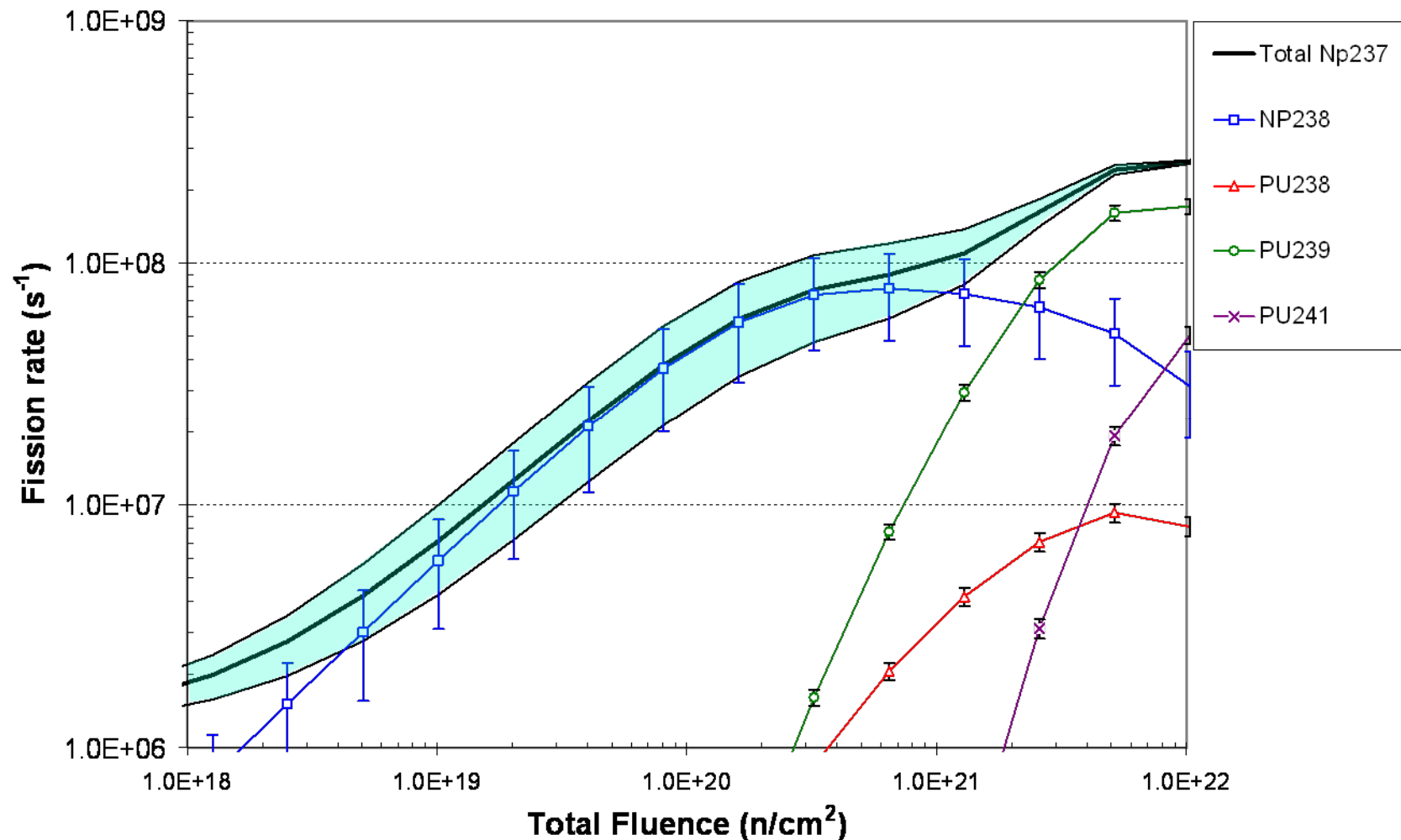
## PART IV: Relative error in fission rates Pu242#1 in BR2

**Figure 11.** Contribution and error bars (one standard deviation) of each isotope in the total fission rate for a deposit of Pu242#2 (see Table I for initial composition) in a typical high flux thermal neutron environment (BR2).



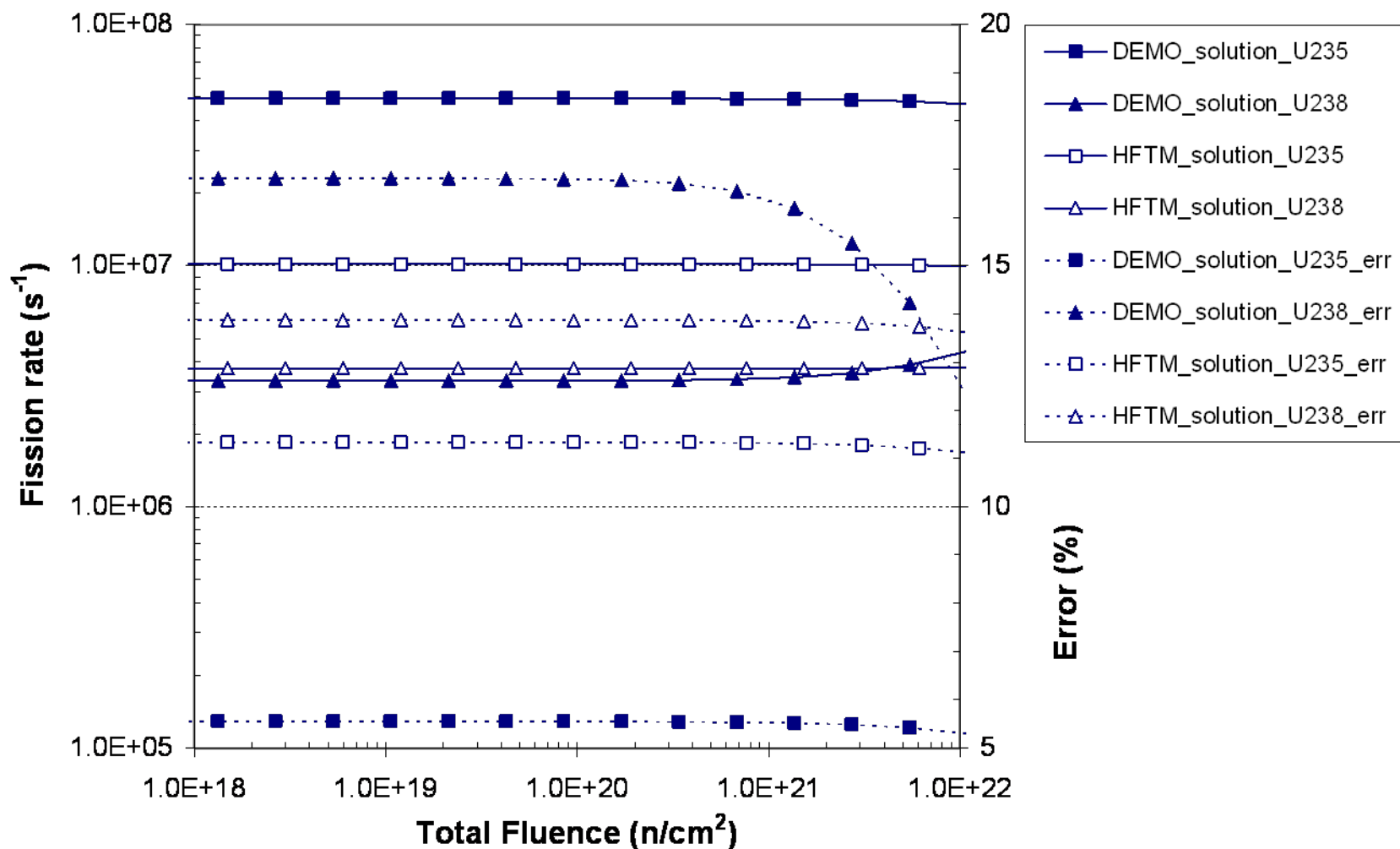
## PART IV: Relative error in fission rates Np237 in BR2

**Figure 12.** Total fission rate and error bars (one standard deviation) for initially pure Np237 deposit irradiated in a high flux thermal environment (e.g. BR2). Contributions of each isotope to the total fission rate and errors are shown.



## PART IV: Relative error in fission rates DEMO/IFMIF

**Figure 13.** Fission rates and relative error (in %) for different U235 and U238 deposits in DEMO and HFTM/IFMIF neutron environments.



# CONCLUSIONS

- ✚ We present an assessment of fissionable material behaviour in three neutron scenarios with different degrees of hardness (BR2, DEMO and IFMIF)
  - ✚ The evolution of fission rates as a function of the fluence for some potential/realistic deposits or solutions are predicted as well as other parameters having influence on the FC behaviour for a long-term performance (sensitivities to fast neutrons, xenon prediction and spectral history effect in BR2 due to changes in temperature)
    - ✚ In BR2, the fission rates are stable with deposits of  $\text{Pu}^{242\#1,2}$  up to fluences as high as  $10^{22} \text{ n/cm}^2$  as well as satisfying high values of  $S_{\text{fast}}$
    - ✚ For DEMO and IFMIF, fission rates remain stable for the complete set of deposits
- ✚ Uncertainty calculation due to uncertainties in activation cross sections (a Monte Carlo technique implemented in ACAB code has been used to propagate ND uncertainties)
  - ✚ In BR2, large uncertainties were found in deposits of  $\text{Np}^{237}$  and  $\text{Pu}^{242}$  due to uncertainties in fission cross sections of  $^{238}\text{Np}$  and  $^{243}\text{Pu}$ , respectively
  - ✚ In addition, we have found that the uncertainty in the contribution of  $^{245}\text{Cm}$  at high fluences in the deposits of  $\text{Pu}^{242}$  is mainly due to the uncertainty in its inventory
  - ✚ For other deposits, uncertainties remain below 5% for fission rates up to fluences of  $10^{22} \text{ n/cm}^2$ .
  - ✚ In the HFTM/IFMIF and DEMO, we found relative errors in fission rates between 5% and 17%
  - ✚ In conclusion, the knowledge of the evolution of these uncertainties can help to better understand the expected responses of fission chambers